

1 **The role of the winter residual circulation in the summer mesopause**  
2 **regions in WACCM**

3 Maartje Sanne Kuilman<sup>1</sup>, Bodil Karlsson<sup>1</sup>

4 <sup>1</sup>Department of Meteorology, Stockholm University, 10691 Stockholm,  
5 Sweden.

6 *Correspondence to:* Maartje Sanne Kuilman (maartje.kuilman@misu.su.se)

7  
8 **Abstract**

9  
10 High winter planetary wave activity warms the summer polar mesopause via a  
11 link between the two hemispheres. In a recent study carried out with the  
12 Kühlungsborn Mechanistic general Circulation Model (KMCM), it was shown  
13 that the net effect of this interhemispheric coupling mechanism is a cooling of  
14 the summer polar mesospheres and that this temperature response is tied to  
15 the strength of the gravity wave-driven winter mesospheric flow. We here  
16 reconfirm the hypothesis that the summer polar mesosphere would be  
17 substantially warmer without the circulation in the winter mesosphere, using  
18 the widely-used Whole Atmosphere Community Climate Model (WACCM). In  
19 addition, the role of the stratosphere in shaping the conditions of the summer  
20 polar mesosphere is investigated. Using composite analysis, we show that if  
21 winter gravity waves are absent, a weak stratospheric Brewer-Dobson  
22 circulation would lead to a warming of the summer mesosphere region instead  
23 of a cooling, and vice versa. This is opposing the temperature signal of the  
24 interhemispheric coupling in the mesosphere, in which a cold winter  
25 stratosphere goes together with a cold summer mesopause. We hereby  
26 strengthen the evidence that the equatorial mesospheric temperature  
27 response, driven by the winter gravity waves, is a crucial step in the  
28 interhemispheric coupling mechanism.

29  
30 **1 Introduction**

31  
32 The circulation in the mesosphere is driven by atmospheric gravity waves  
33 (GWs). These waves originate from the lower atmosphere and as they  
34 propagate upwards, they are filtered by the zonal wind in the stratosphere  
35 (e.g., Fritts and Alexander, 2003). Because of the decreasing density with

36 altitude and as a result of energy conservation, the waves grow in amplitude.  
37 At certain altitudes, the waves – depending on their phase speeds relative to  
38 the background wind - become unstable and break. At the level of breaking,  
39 the waves deposit their momentum into the background flow, creating a drag  
40 on the zonal winds in the mesosphere, which establishes the pole-to-pole  
41 circulation (e.g. Lindzen, 1981; Holton, 1982,1983; Garcia and Solomon,  
42 1985). This circulation drives the temperatures far away from the state of  
43 radiative balance, by adiabatically heating the winter mesopause and  
44 adiabatically cooling the summertime mesopause (Andrews et al., 1987;  
45 Haurwitz, 1961; Garcia and Solomon, 1985; Fritts and Alexander, 2003). The  
46 adiabatic cooling in the summer leads to temperatures sometimes lower than  
47 130 K in the summer mesopause (Lübken et al.,1990). These low  
48 temperatures allow for the formation of thin ice clouds in the summer  
49 mesopause region, the so-called noctilucent clouds (NLCs).

50  
51 Previous studies have shown that the summer polar mesosphere is influenced  
52 by the winter stratosphere via a chain of wave-mean flow interactions (e.g.  
53 Becker and Schmitz, 2003; Becker et al., 2004; Karlsson et al., 2009). This  
54 phenomenon, termed interhemispheric coupling (IHC), manifests itself as an  
55 anomaly of the zonal mean temperatures. Its pattern consists of a quadruple  
56 structure in the winter hemisphere with a warming (cooling) of the polar  
57 stratosphere and an associated cooling (warming) in the equatorial  
58 stratosphere. In the mesosphere, these anomalies are reversed: there is a  
59 cooling (warming) in the polar mesosphere, and an associated warming  
60 (cooling) in the equatorial region. The mesospheric warming (cooling) in the  
61 tropical region extends to the summer mesopause (see e.g. Körnich and  
62 Becker, 2010).

63  
64 These anomalies are responses to different wave forcing in the winter  
65 hemisphere. To understand how these anomalies come about we have to  
66 understand the interhemispheric coupling mechanism. The mechanism, as  
67 discussed here, is for the case of a stronger winter residual circulation, but  
68 works the same for a weakening of this circulation (Karlsson et al., 2009).  
69 A stronger planetary wave (PW) forcing in the winter stratosphere yields a

70 stronger stratospheric Brewer-Dobson circulation (BDC). This anomalously  
71 strong flow yields an anomalously cold stratospheric tropical region and a  
72 warm stratospheric winter pole, due to the downward control principle  
73 (Haynes et al. 1991).

74

75 Due to the eastward zonal flow in the winter stratosphere, GWs carrying  
76 westward momentum propagate relatively freely up through the mesosphere  
77 where they break. Therefore, in the winter mesosphere, the net drag from  
78 GWs momentum deposition is westward. When vertically propagating  
79 planetary waves break – also carrying westward momentum – in the  
80 stratosphere, the momentum deposited onto the mean flow decelerates the  
81 stratospheric westerly winter flow. To put it short, a weaker zonal  
82 stratospheric winter flow allows for the upward propagation of more GWs with  
83 an eastward phase speed, which, as they break reduces the westward wave  
84 drag (see Becker and Schmitz, 2003, for a more rigorous description).

85

86 This filtering effect of the zonal background flow on the GW propagation  
87 results in a reduction in strength of the winter-side mesospheric residual  
88 circulation when the BDC is stronger. The downward control principle now  
89 causes the mesospheric polar winter region to be anomalously cold and the  
90 tropical mesosphere to be anomalously warm (Becker and Schmitz, 2003,  
91 Becker et al., 2004; Körnich and Becker, 2009).

92

93 The critical step for IHC is the crossing of the temperature signal over the  
94 equator. The essential region is here the equatorial mesosphere. Central in  
95 the hypothesis of IHC is that the increase (or decrease) of the temperature in  
96 the tropical mesosphere modifies the temperature gradient between high and  
97 low latitudes in the summer mesosphere, which influences the zonal wind in  
98 the summer mesosphere, due to thermal wind balance (see e.g. Karlsson et  
99 al., 2009 and Karlsson and Becker, 2016).

100

101 The zonal wind change in the summer mesosphere modifies the breaking  
102 level of the summer-side GWs. In the case of a warming in the equatorial  
103 mesosphere – as when the BDC is strong -, the zonal wind is modified in such

104 a way that the intrinsic wave speeds are reduced (e.g. Becker and Schmitz,  
105 2003; Körnich and Becker, 2009). When the relative speed between the GWs  
106 and the zonal flow decreases, the GWs break at a lower altitude, thereby  
107 shifting down the GW drag per unit mass. The upper branch of the residual  
108 circulation also shifts downwards and along with this shift there is a reduction  
109 of adiabatic cooling, which causes a positive temperature anomaly in the  
110 summer mesosphere (Karlsson et al., 2009; Körnich and Becker, 2009;  
111 Karlsson and Becker, 2016). In the case of an equatorial mesospheric cooling,  
112 the response is the opposite: the relative difference between the zonal flow  
113 and the phase speeds of the gravity waves increase to that they break at a  
114 slightly higher altitude, with an anomalous cooling of the summer mesopause  
115 as a result.

116

117 The IHC pattern was first found using mechanistic models (Becker and  
118 Schmitz, 2003; Becker et al., 2004; Becker and Fritts, 2006), underpinned by  
119 observations of mesospheric conditions. The pattern was then found in  
120 observational data (e.g. Karlsson et al., 2007; Gumbel and Karlsson, 2011;  
121 Espy et al., 2011; de Wit et al., 2016), in the Whole Atmosphere Community  
122 Climate Model (WACCM: Sassi et al. 2004, Tan et al., 2012), in the Canadian  
123 Middle Atmosphere Model (CMAM: Karlsson et al. 2009), and in the high  
124 altitude analysis from the Navy Operational Global Atmospheric Prediction  
125 System- Advanced Level Physics High Altitude (NOGAPS-ALPHA)  
126 forecast/assimilating system (Siskind et al., 2011).

127

128 We saw that the temperature in the equatorial mesosphere is modified by the  
129 strength of the residual circulation in the winter mesosphere. Karlsson and  
130 Becker (2016) hypothesized that if the GW-driven winter residual circulation  
131 would not be present, the equatorial mesosphere would be warmer, which  
132 would lead to lower breaking levels of GWs in the summer hemisphere and a  
133 warmer summer mesosphere region. Analogically, an anomalously cold  
134 equatorial region would lead to an anomalously cold summer mesosphere  
135 region (e.g. Karlsson et al., 2009; Karlsson and Becker, 2016).

136

137 Becker and Karlsson (2016) showed that the equatorial mesosphere is

138 substantially colder in July than it is in January, while the winter mesosphere  
139 is significantly warmer (see their Fig. 1). That means that the GWs break  
140 higher in the NH summer mesosphere than in the SH summer mesosphere,  
141 which is one possible reason for why the July summer polar mesosphere is  
142 colder than in the January summer polar mesosphere (e.g. Becker and Fritts,  
143 2006; Karlsson et al., 2009). If – as hypothesized by Karlsson and Becker  
144 (2016) – the fundamental effect of the IHC is a cooling of the summer  
145 mesopauses, it would mean that the mechanism plays a more important role  
146 affecting the temperatures in the summer mesopause in the NH compared to  
147 that in the SH, since the weaker planetary wave activity in the SH results in an  
148 increased gravity wave drag and a strengthening of mesospheric poleward  
149 flow in the winter mesosphere. The equatorial mesosphere is adiabatically  
150 cooled more efficiently than when the winter mesospheric circulation is weak.  
151

152 Karlsson and Becker (2016) hypothesized that in the absence of the equator-  
153 to-pole flow in the SH winter, the summer mesopause in the NH would be  
154 considerably warmer. Moreover, removing the mesospheric residual  
155 circulation in the NH winter would not have as high impact on the SH summer  
156 mesopause. To test the hypothesis, they used the KMCM to compare control  
157 simulations to runs without GWs in the winter mesosphere. The predicted  
158 responses were confirmed, and the results were also backed up by correlation  
159 studies using the Canadian Middle Atmosphere Model (CMAM30).  
160

161 Since IHC is controversial, we find it important to use as many tools as  
162 possible to test – and to underpin - our arguments. In this study, the well-  
163 established WACCM, described in section 2.1 below, is used to endorse the  
164 results obtained with the not as widely-used – yet high-performing – KMCM.  
165 WACCM is in some aspects a more comprehensive model than KMCM. For  
166 example, a major difference is that WACCM contains interactive chemistry in  
167 the middle atmosphere, while KMCM does not. WACCM also uses a different  
168 parameterization for non-orographic GWs than KMCM. KMCM uses a  
169 simplified dynamical core and convection scheme as compared to WACCM.  
170 For details about the KMCM see e.g. Becker et al., 2015. The WACCM is  
171 described in section 2.

172 In section 3, we discuss the effect of removing the gravity waves in the winter  
173 hemisphere on the summer mesosphere region in WACCM. We also  
174 investigate the consequences for noctilucent clouds, formed in the  
175 mesopause region. Therefore, we implement a basic cloud parameterization,  
176 as described in Section 2.2. The Whole Atmosphere Community Climate  
177 Model (WACCM) results from comparing runs with and without winter GWs  
178 are presented in Section 3.

179

180 As an important complement to the study carried out by Karlsson and Becker  
181 (2016), we here examine the role of the summer stratosphere in shaping the  
182 conditions of the NH summer polar mesosphere when the winter mesospheric  
183 flow is absent. We focus on the effect that the zonal wind in the summer  
184 stratosphere has, and study if and how the PW activity in the winter affects  
185 the summer polar mesosphere. These results are presented in Section 3.1.

186

187 Our conclusions are summarized in Section 4. Since the IHC mechanism has  
188 a more robust signal in the SH winter – NH summer, we choose to focus  
189 particularly on this period, namely July. Nevertheless, results from January  
190 are also shown for comparisons and for further discussion.

191

## 192 **2 Method**

193

### 194 **2.1 Model**

195

196 The Whole Atmosphere Community Climate Model (WACCM) is a so-called  
197 “high-top” chemistry-climate model, which spans the range of altitude from the  
198 Earth’s surface to an altitude of about 140 km. WACCM has 66 vertical levels  
199 of a resolution of ~1.1 km in the troposphere above the boundary layer, 1.1-  
200 1.4 km in the lower stratosphere, 1.75 km at the stratosphere and 3.5 km  
201 above 65 km. The horizontal resolution is 1.9° latitude by 2.5° longitude  
202 (Marsh et al, 2013).

203

204 The model is a component of the Community Earth System Model (CESM),  
205 which is a group of model components at the National Center for Atmospheric

206 Research (NCAR). WACCM is a superset of the Community Atmospheric  
207 Model version 4 (CAM4) and as such it includes all the physical  
208 parameterizations of CAM4 (Neale et al., 2013).

209

210 WACCM includes parameterized non-orographic gravity waves, which are  
211 generated by frontal systems and convection (Richter et al., 2010). The  
212 orographic GW parameterization is based on McFarlane (1987), while the  
213 nonorographic GW propagation parameterization is based the formulation by  
214 Lindzen (1981).

215

216 In this study, The F\_2000\_WACCM (FW) compset of the model is used, i.e.  
217 the model assumes present day conditions. There is no forcing applied: the  
218 model runs a perpetual year 2000. Our results are based on a control run and  
219 perturbation runs. In the control run, the winter side residual circulation is  
220 included. In the perturbation runs, the equator-to-pole flow is removed by  
221 turning off both the orographic and the non-orographic gravity waves. It  
222 should however be noted that even though the GWs are turned off, there are  
223 still some resolved waves, such as inertial gravity waves and planetary waves  
224 that drive a weak meridional circulation. The model is run for 30 years.

225

### 226 **3 Results and discussion**

227 To investigate the effect of the winter residual circulation on the summer  
228 mesopause, we compare the control run, which includes the winter equator-  
229 to-pole circulation, with the perturbation runs. In the perturbation runs, the  
230 equator-to-pole flow is removed by turning off the parameterized gravity  
231 waves in the winter hemisphere. The resolved waves, such as tides, inertial  
232 gravity waves and planetary waves are still there and drive a weak poleward  
233 flow, as already described in section 2.1.

234 We start by investigating the case for the NH summer (July) with the GWs  
235 turned off for the SH, where it is winter. Figure 1 shows the difference in  
236 zonal-mean temperature, zonal wind and gravity wave drag for July as a  
237 function of latitude and altitude, between the control run and the perturbation

238 run: the run without the GWs in the winter minus the run with the GWs in the  
239 SH.

240 Figure 1.

241 From Fig. 1, it is clear that there is a considerable increase in temperature in  
242 the NH summer mesopause region in the case for which there is no equator-  
243 to-pole flow in the SH winter. This change in temperature in the summer polar  
244 mesosphere can be understood as a result of changes in the wave-mean flow  
245 interactions. Without the GWs in the SH winter, the winter stratosphere and  
246 lower mesosphere are colder. This is because GWs in the winter hemisphere  
247 drive downwelling, adiabatically heating these regions (e.g. Karlsson et al.,  
248 2009).

249 From Fig. 1 it can also be seen that there is a significant warming in the  
250 equatorial stratosphere in the case where there are no GWs in the winter  
251 hemisphere, indicating a weakening of the BDC. We suggest that this could  
252 be due to a redistribution of PW momentum drag in the winter stratosphere:  
253 as the zonal flow is no longer reversed in the mesosphere by GW-drag, the  
254 breaking levels of the westward propagating planetary waves are shifted  
255 upwards. Hence, the PW drag could be distributed over a wider altitude range.  
256 Another contributor to a decrease in the BDC is the removal of the orographic  
257 GWs, which act as PWs on the zonal flow in the winter stratosphere (see e.g.  
258 Karlsson and Becker, 2016; their figure 7).

259 Turning off the gravity waves in winter hemisphere, changes the meridional  
260 temperature gradient in the winter hemisphere, as the equatorial mesosphere  
261 will be warmer. This tropical temperature response changes the meridional  
262 temperature gradient in the summer mesosphere, and thereby – via thermal  
263 wind balance - the zonal mesospheric winds: the westward jet will be weaker.  
264 It is also clear that the zonal flow at high latitudes accelerates for the case for  
265 which there is no equator-to-pole flow in the SH winter. These findings  
266 correspond with what is found in Karlsson and Becker (2016).

267 The weaker jet leads in turn to lower GW levels and weaker GW drag over  
268 45°N-70°N above a pressure level of 0.02 hPa as can be seen in Fig. 1. This



269 causes the summer polar mesopause to be considerably warmer. The  
270 temperature increase in the summer polar mesopause region, which is now  
271 loosely defined to be between 61°N - 90°N and 0.01 - 0.002 hPa, is  
272 approximately 16 degrees. In a radiation-driven atmosphere the temperature  
273 in the NH NLC region is about 210-220 K, much higher than the temperature  
274 both with and without the GWs in the SH.

275 When we compare our results with the results in Karlsson and Becker (2016,  
276 their figure 3), we observe there are some quantitative discrepancies in the  
277 structure of the responses. For example, Karlsson and Becker (2016) found  
278 that removing the winter GWs resulted in a warming of the mesosphere  
279 globally, although the response was strongest in the polar mesopause region.  
280 They attributed that the warming over the equatorial and winter mesosphere  
281 to the effect that GWs have on tides: when GWs are absent, the tidal  
282 response is enhanced. The same behavior is not found in WACCM - in fact,  
283 the equatorial upper mesosphere is anomalously cooler when the GWs are  
284 removed. These differences could perhaps be explained by for example the  
285 different gravity wave parameterization of non-orographic GWs, the different  
286 dynamical cores between the models and the presence of interactive  
287 chemistry in the middle atmosphere in WACCM. However, the qualitative  
288 response of the temperature and zonal wind change due to turning of the  
289 GWs in the SH corresponds well with the results from the KMCM as well as  
290 with our hypothesis.

291 It can also be seen that like in the KMCM model, the zonal wind and  
292 temperature in summer stratosphere region change only slightly in the  
293 perturbation runs as compared to the control runs. We deem that anomalous  
294 GW filtering effects from the lower down in the summer stratosphere, which  
295 could affect the results, are unlikely to contribute substantially to the  
296 temperature change in the summer mesosphere. We come back to this  
297 question in the next paragraph 3.1.

298 To investigate the IHC mechanism further, we also show the correlation and  
299 covariance, which also provides information about the amplitude of the  
300 variability, between the temperature in the winter stratosphere in July (1-10

301 hPa, 60°S-40°S) and the temperatures in the rest of the atmosphere in the  
302 same month. The latitude and altitude ranges chosen for July is the region  
303 where the SH winter stratosphere variability is best captured (see Karlsson  
304 and Becker, 2016; their figure 9). This is related to the relatively weak PW  
305 forcing in the SH – the BDC is not reaching all the way to the polar region  
306 (Kuroda and Kodera, 2001).

307 We show the correlation and covariance fields for both the cases with and  
308 without GWs in the SH winter hemisphere.

309 Figure 2

310 In the correlation and covariance fields of the control run, the temperature in  
311 the winter stratosphere is positively correlated with the temperature in the  
312 equatorial mesosphere and the summer mesopause region. Comparing the  
313 results show in Figure 2 (upper left) to Figure 8e in Karlsson and Becker  
314 (2016), it can be seen that the correlation coefficients are of similar  
315 magnitudes, but the spatial responses differ in altitude and in latitudinal  
316 extent: whereas the correlation signal is significant in the CMAM30 July high  
317 latitude summer mesopause, the WACCM July response reaches only the  
318 lowermost latitudes (about 50°N in latitude).

319

320 If the GWs are removed in the winter hemisphere, the temperature in the  
321 summer mesopause region anti-correlates with the temperature in the winter  
322 stratosphere. Also, the temperature in the equatorial mesosphere does no  
323 longer correlate and co-vary significantly with the temperature in the winter  
324 hemisphere, in agreement with the results of Karlsson and Becker (2016).

325 Until now, we investigated the influence of the SH winter residual circulation  
326 on the NH summer mesopause in July. Now, we will also investigate the  
327 effect that the NH winter residual circulation has on the SH summer  
328 mesosphere in January. We discussed earlier that this effect will be smaller  
329 as compared to the effect of the SH winter residual circulation on the NH  
330 summer mesosphere in July. Figure 3 shows the difference in zonal-mean  
331 temperature, zonal wind and gravity wave drag for January as a function of

332 latitude and altitude, between the control run and the perturbation run: the run  
333 without the GWs in the NH winter hemisphere minus the run with the GWs in  
334 the NH winter hemisphere (similar to Fig. 1).

335 Figure 3.

336 From Fig. 3, it can be observed that there is no statistically significant  
337 temperature change in the SH summer polar mesopause region in the case  
338 for which there is no equator-to-pole flow in the NH winter. Without the GWs  
339 in the winter hemisphere, the winter stratosphere and lower mesosphere are  
340 colder, as in the July case. There is a change in zonal wind at high southern  
341 latitudes, but there is no clear statistical significant increase. These findings  
342 correspond with what is hypothesized in the introduction: taking away the  
343 GWs in the NH winter will have a less effect on the SH summer mesopause  
344 than taking away the GWs in the SH winter on the NH summer mesopause.

345 This is due to the variable nature of the winter stratosphere zonal flow in the  
346 NH, which oscillates between being weak and strong. As a result, the January  
347 equatorial mesosphere is modified continuously: it varies between being  
348 cooled and warmed by the winter mesospheric residual flow. In July, on the  
349 other hand, the equatorial region is continuously cooled by the strong  
350 mesospheric residual flow in the SH winter. Hence, the interhemispheric  
351 coupling mechanism gives a plausible explanation to why the July summer  
352 mesosphere region is considerably colder than the one in January.

353 Comparison between the responses found using WACCM with those found  
354 with KMCM (Karlsson and Becker, 2016, their Fig. 3), shows that the  
355 temperature change is larger and extends all the way to the summer pole in  
356 KMCM, while this is not the case in WACCM. Moreover, the change in  
357 temperature in this region is not statically significant in WACCM. The  
358 differences in temperature and zonal wind responses are larger in January  
359 than in July when comparing the results of WACCM with that of KMCM.  
360 Nevertheless, the qualitative structure of the temperature and zonal wind  
361 change due to turning of the winter GWs corresponds convincingly well.

362 In Fig. 4, we show the correlation and covariance between the temperature in  
363 the winter stratosphere in January (1-10 hPa, 60°N-80°N) and the  
364 temperatures in the rest of the atmosphere in the same month for both the  
365 cases with and without GWs in the NH winter hemisphere.

366 Figure 4

367 The general pattern in January for the correlation and covariance for both the  
368 control run and the run without GWs in the winter hemisphere is very similar  
369 to the pattern in July. However, the correlation and covariance in the summer  
370 mesosphere with the temperatures in the winter stratosphere are not  
371 statistically significant. This can be understood, as the variability in the SH  
372 summer mesopause region in January is much higher. It is seen that in both  
373 hemispheres, the temperature in the equatorial mesosphere correlates  
374 statistically significant with the temperatures in the winter stratosphere for the  
375 control case, but not for the case without the GWs in the winter hemisphere.

376 IHC has hitherto primarily been seen as a mode of internal variability giving  
377 rise to a warming of the summer polar mesopause region. These results  
378 presented here and in Karlsson and Becker (2016) show the more  
379 fundamental role of interhemispheric coupling; the mechanism has a net  
380 cooling effect on the summer polar mesosphere. This study reconfirms this  
381 fundamental role of the IHC mechanism and strengthens the evidence that  
382 the equatorial mesospheric temperature response is the crucial step in the  
383 interhemispheric coupling mechanism.

384

### 385 **3.1 The role of the summer stratosphere region**

386 The BDC is modifying in the summer stratospheric meridional temperature  
387 gradient. Hence, filtering effects taking place below the mesosphere may  
388 seem like an additional - or alternative – mechanism to the response  
389 observed in the summer mesopause. In this section, we will discuss why this  
390 cannot be the case. We focus again mostly on the NH summer polar  
391 mesosphere region.

392

393 In Fig. 1, it is seen that if there are GWs in the SH winter hemisphere the  
394 temperature in the winter stratosphere is positively correlated with the  
395 temperature in the NH summer polar mesosphere. This means that for a  
396 stronger Brewer-Dobson circulation (BDC) and the resulting anomalously  
397 warm (cold) temperatures in the stratosphere at 40°- 60°S, there will be also  
398 an anomalously warm (cold) temperature in the summer polar mesosphere.  
399

400 A strong or weak BDC results in a temperature change in the equatorial  
401 mesosphere, which changes the meridional temperature gradient in the  
402 summer mesosphere. As a result of the change in strength of the BDC, there  
403 is a change in the meridional temperature gradient as well, however, this  
404 gradient will have an opposite sign, as can be seen from Fig 1. As pointed out  
405 by Karlsson et al. (2009), the expected GW filtering effect of this stratospheric  
406 temperature gradient would oppose that of the mesospheric temperature  
407 gradient.

408

409 This can be shown clearly with the mesospheric winter residual circulation  
410 being out of play. From Fig. 2, it can be seen that anomalously low  
411 temperatures in the SH winter stratosphere, indicating a weak Brewer-Dobson  
412 circulation, without the GWs in the winter lead to a warming in the NH summer  
413 mesopause region, instead of a cooling as observed in the case where there  
414 are GWs in the SH winter hemisphere.

415

416 We hypothesize that this opposing signal is – in the absence of a  
417 mesospheric residual flow in the winter - caused by a modulation of the  
418 meridional temperature gradient in the summer stratosphere, inferred by the  
419 BDC.

420 To strengthen our arguments, we plot the vertical profiles of the zonal wind,  
421 GW drag between 45°N-55°N and the temperatures between 70°N-90°N in  
422 July. These profiles are shown for both high and low temperatures in the  
423 winter stratosphere (1-10 hPa, 60°S-40°S). The differences between the  
424 cases with anomalously low and high temperatures are also plotted.

425 Figure 5

426 From Fig. 5, it is clear for a weak Brewer-Dobson circulation, and therefore  
427 anomalously low temperatures in the SH winter stratosphere, the zonal winds  
428 in the stratosphere are less strongly westwards. This leads to a weaker GW  
429 drag and a warmer NH summer mesopause region.

430 We hereby suggest that without GWs in the SH winter hemisphere, it would  
431 be the variability in the NH summer stratosphere caused by the winter-side  
432 BDC that would have the major influence on the temperatures in the NH  
433 summer mesopause. A weaker (stronger) Brewer-Dobson circulation would  
434 lead to a change in the temperature gradient in the summer stratopause,  
435 which would lead to a cooling (warming) instead of the warming (cooling)  
436 associated with interhemispheric coupling.

437 The same is true for the effect of the SH summer stratosphere on the SH  
438 summer mesosphere in January. The profiles for the southern hemisphere in  
439 January are very similar to the profiles for the northern hemisphere in July,  
440 see figure 6.

441 Figure 6.

442 This means that in both the northern and summer hemisphere, a weaker  
443 (stronger) Brewer-Dobson circulation leads to a change in the temperature  
444 gradient in the summer stratopause, which leads to a warming (cooling)  
445 instead of the cooling (warming) that is associated with interhemispheric  
446 coupling.

#### 447 **4 Conclusions**

448 In this study, the interhemispheric coupling mechanism and the role of the  
449 summer stratosphere in shaping the conditions of the summer polar  
450 mesosphere have been investigated. We have used the widely used WACCM  
451 model to reconfirm the hypothesis of Karlsson and Becker (2016) that the  
452 summer polar mesosphere would be substantially warmer without the gravity  
453 wave-driven residual circulation in the winter. We find, in accordance with the

454 previous study, that the interhemispheric coupling mechanism has a net  
455 cooling effect on the summer polar mesospheres. We also find that the  
456 mechanism plays a more important role affecting the temperatures in the  
457 summer mesopause in the NH compared to that in the SH.

458

459 We have also investigated the role of the summer stratosphere in shaping the  
460 conditions of the summer polar mesosphere. It is shown that without the  
461 winter mesospheric residual circulation, the variability in the summer polar  
462 mesosphere is determined by the temperature gradient in the summer  
463 stratosphere below, which is modulated by the strength of the BDC. We have  
464 found that for both the northern and the southern hemisphere, in the absence  
465 of winter gravity waves, a weak Brewer-Dobson circulation would lead to a  
466 warming of the summer mesosphere region. The temperature signal of the  
467 interhemispheric coupling mechanism is opposite: in this case a weak Brewer-  
468 Dobson circulation, the summer mesosphere region is cooled. This confirms  
469 the idea that it is the equatorial mesosphere that is governing the  
470 temperatures in the summer mesopause regions, rather than processes in the  
471 summer stratosphere.

472

473

474

475

476

477

478

479

480

481

482

483

484

485

486

487

488

489

490

491

492

493

494

495 **References**

496

497 Andrews, D.G., Holton, J.R., Leovy, C.B.: Middle atmosphere dynamics,  
498 Academic Press, United States of America, 1987.

499

500 Becker E. and Fritts, D.C.: Enhanced gravity-wave activity and  
501 interhemispheric coupling during the MaCWAVE/MIDAS northern summer  
502 program 2002, *Ann. Geophys.*, 24, 1175-1188, doi:10.5194/angeo-24-1175-  
503 2006, 2006.

504

505 Becker, E. and Schmitz, G.: Climatological effects of orography and land-sea  
506 contrasts on the gravity wave-driven circulation of the mesosphere, *J. Atmos.*  
507 *Sci.*, 60, 103-118, doi:.1175/1520-0469(2003)060<0103:CEOOAL>2.0.CO;2,  
508 2003.

509

510 Becker, E., R. Knöpfel and F.-J. Lübken, 2015: Dynamically induced  
511 hemispheric differences in the seasonal cycle of the summer polar  
512 mesopause. *J. Atmos. Solar-Terr. Phys.*, 129, 128-141,  
513 doi:10.1016/j.jastp.2015.04.014.

514

515 Becker, E., Müllermann, A., Lübken, F.-J., Körnich, H., Hoffmann, P., Rapp,  
516 M.: High Rossby-wave activity in austral winter 2002: Modulation of the  
517 general circulation of the MLT during the MaCWAVE/MIDAS northern summer  
518 program, *Geophys. Res. Lett.*, 31, L24S03, doi:10.1029/2004GL019615, 2004.

519 Christensen, O.M., Benze, S., Eriksson, P., Gumbel, J., Megner, L., Murtagh,  
520 D.P.: The relationship between Polar Mesospheric Clouds and their  
521 background atmosphere as observed by Odin-SMR and Odin-OSIRIS, *Atmos.*  
522 *Chem. Phys.*, 16, 12587-12600, doi:10.5194/acp-16-12587-2016, 2016.

523 De Wit, R.J., Janches, D., Fritts, D.C., Hibbins, R.E.: QBO modulation of the  
524 mesopause gravity wave momentum flux over Tierra del Fuego, *Geophys.*  
525 *Res. Lett.*, 43, 4094-4055, doi:10.1002/2016GL068599, 2016.

526

527 Espy, P.J., Ochoa Fernández, S., Forkman, P., Murtagh, D., Stegman, J.:



528 The role of the QBO in the inter-hemispheric coupling of summer mesospheric  
529 temperatures, *Atmos. Chem. Phys.*, 11, doi:10.5194/acp-11-495-2011, 495-  
530 502, 2011.

531

532 Fritts, D. C. and Alexander, M.J.: Gravity wave dynamics and effects in the  
533 middle atmosphere, *Rev. Geophys.*, 41, 1003, doi:10.1029/2001RG000106,  
534 2003.

535

536 Garcia, R.R., Solomon, S.: The effect of breaking gravity waves on the  
537 dynamics and chemical composition of the mesosphere and lower  
538 thermosphere, *J. Geophys. Res.*, 90, D2, 3850-3868,  
539 10.1029/JD090iD02p03850, 1985.

540

541 Gumbel, J., Karlsson, B.: Intra- and inter-hemispheric coupling effects on the  
542 polar summer mesosphere, *Geophys. Res. Lett.*, 38, L14804,  
543 doi:10.1029/2011GL047968, 2011.

544

545 Haurwitz, B.: Frictional effects and the meridional circulation in the  
546 mesosphere, *J. Geophys. Res.*, 66, 8, doi:10.1029/JZ066i008p02381, 1961.

547

548 Haynes, P.H., Marks, C.J., McIntyre, M.E., Shepherd, T.G., Shine, K.P.: On  
549 the “downward control” of extratropical diabatic circulations by eddy-induced  
550 mean zonal forces, *J. Atmos. Sci.*, 48, 651-678, 10.1175/1520-  
551 0469(1991)048<0651:OTCOED>2.0.CO;2, 1991.

552 Hervig, M.E., Stevens, M.H., Gordley, L.L., Deaver, L.E., Russell, J.M., Bailey,  
553 S.M.: Relationships between polar mesospheric clouds, temperature, and  
554 water vapor from Solar Occultation for Ice Experiment (SOFIE) observations,  
555 *J. Geophys. Res.*, 114, D20203, doi:10.1029/2009JD012302, 2009.

556 Holton, J.R.: The role of gravity wave induced drag and diffusion in the  
557 momentum budget of the mesosphere, *J. Atmos. Sci.*, 39, 791-799,  
558 doi:10.1175/1520-0469(1982)039<0791:TROGWI>2.0.CO;2, 1982.

559

560 Holton, J.R.: The influence of gravity wave breaking on the general circulation  
561 of the middle atmosphere, *J. Atmos. Sci.*, 40, 2497-2507, doi:10.1175/1520-  
562 0469(1983)040<2497:TIOGWB>2.0.CO;2, 1983.

563

564 Karlsson, B., Körnich, H., Gumbel, J.: Evidence for interhemispheric  
565 stratosphere-mesosphere coupling derived from noctilucent cloud properties,  
566 *Geophys. Res. Lett.*, 34, L16806, doi:10.1029/2007GL030282, 2007.

567

568 Karlsson, B., McLandress, C., Shepherd, T.G.: Inter-hemispheric mesospheric  
569 coupling in a comprehensive middle atmosphere model, *J. Atmos. Sol.-Terr.*  
570 *Phys.*, 71, 3-4, 518-530, doi:10.1016/j.jastp.2008.08.006, 2009.

571

572 Karlsson, B., Becker, E.: How does interhemispheric coupling contribute to  
573 cool down the summer polar mesosphere?, 29, 8807-8821, doi:10.1175/JCLI-  
574 D-16-0231.1, *J. Climate*, 2016.

575

576 Körnich, H. and Becker, E.: A simple model for the interhemispheric coupling  
577 of the middle atmosphere circulation, *Adv. in Space Res.*, 45, 5, 661-668,  
578 doi:10.1016/j.asr.2009.11.001, 2010.

579

580 Kuroda, Y., and K. Kodera: Variability of the polar night jet in the Northern and  
581 Southern Hemispheres, *J. Geophys. Res.*, 106(D18),20,703–20, 713, 2001.

582

583 Lindzen, R.S.: Turbulence stress owing to gravity wave and tidal breakdown,  
584 *J. Geophys. Res.*, 86, C10, 9707-9714, 10.1029/JC086iC10p09707, 1981.

585

586 Lübken, F.-J., Von Zahn, U., Manson, A., Meek, C., Hoppe, U.-P., Schmidlin,  
587 F.J., Stegman, J., Murtagh, D.P., Rüster, R., Schmitz, G., Widdel, H.-U., Espy,  
588 P.: Mean state densities, temperatures and winds during the MAC/SINE and  
589 MAC/EPSILON campaigns, *J. Atmos. Sol.-Terr. Phys.*, 52, 10-11, 955-970,  
590 [https://doi.org/10.1016/0021-9169\(90\)90027-K](https://doi.org/10.1016/0021-9169(90)90027-K), 1990.

591 Richter, J. H., Sassi, F., Garcia, R.R.: Toward a physically based gravity wave  
592 source parameterization in a general circulation model, *J. Atmos. Sci.*, 67,  
593 136–156, DOI: 10.1175/2009JAS3112.1, 2010.

594 Rong, P., Russell, J. M., Gordley, L. L., Hervig, M. E., Deaver, L., Bernath, P.  
595 F., Walker, K. A.: Validation of v1.022 mesospheric water vapor observed by  
596 the Solar Occultation for Ice Experiment instrument on the Aeronomy of Ice in  
597 the Mesosphere satellite, *J. Geophys. Res.*, 115, D24314,  
598 doi:10.1029/2010JD014269, 2010.

599

600 Marsh, D. R., Mills, M.J., Kinnison, D.E., Lamarque, J.F., Calvo, N., Polvani,  
601 L.M.: Climate change from 1850 to 2005 simulated in CESM1(WACCM),  
602 73727391, *J. Climate*, 26, 19, doi:10.1175/JCLI-D-12-00558.1, 2013.

603 McFarlane, N. A.: The effect of orographically excited wave drag on the  
604 general circulation of the lower stratosphere and troposphere, *J. Atmos. Sci.*,  
605 44, 1775–1800, 10.1175/1520-0469(1987)044<1775:TEOOEG>2.0.CO;2,  
606 1987.

607 Megner, L.: Minimal impact of condensation nuclei characteristics on  
608 observable mesospheric ice properties, *J. Atmos. Sol.-Terr. Phys*, 73, 14-15,  
609 2184-2191, doi:10.1016/j.jastp.2010.08.006, 2011.

610

611 Merkel, A.W., Marsh, D.R., Gettelman, A., Jensen, E.J: On the relationship of  
612 polar mesospheric cloud ice water content particle radius and mesospheric  
613 temperature and its use in multi-dimensional model, *Atmos. Chem. Phys.*, 9,  
614 8889-8901, doi:10.5194/acp-9-8889-2009, 2009.

615

616 Murphy, D. M. and Koop, T.: Review of the vapor pressure of ice and super-  
617 cooled water for atmospheric applications, *Q. J. R. Meteorol. Soc.*, 131, 1539-  
618 1565, doi:10.1256/qj.04.94, 2005.

619 Neale, R., Richter, J., Park, S., Lauritzen, P., Vavrus, S., Rasch, P., Zhang,  
620 M.: The mean climate of the Community Atmosphere Model (CAM4) in forced

621 SST and fully coupled experiments, *J. Climate*, 26, 5150–5168,  
622 doi:10.1175/JCLI-D-12-00236.1, 2013.

623 Sassi, F., Kinnison, D., Boville, B.A., Garcia, R.R., Roble, R.: Effect of El  
624 Niño- Southern Oscillation on the dynamical, thermal, chemical structure of  
625 the middle atmosphere, *J. Geophys. Res.*, 109, D17108,  
626 doi:10.1029/2003JD004434, 2004.

627

628 Siskind, D. E., Stevens, M.H., Hervig, M., Sassi, F., Hoppel, K., Englert, C.R.,  
629 Kochenas, A.J., Consequences of recent Southern Hemisphere winter  
630 variability on polar mesospheric clouds, *J. Atmos. Sol. Terr. Phys.*, 73, 2013–  
631 2021, 10.1016/j.jastp.2011.06.014, 2011.

632

633 Tan, B., Chu, X., Liu, H.-L.: Yamashita, C., Russell III, J.M.: Zonal-mean  
634 global teleconnections from 15 to 110 km derived from SABER and WACCM,  
635 *J. Geophys. Res.*, 117, D10106, doi:10.1029/2011JD016750, 2012.

636

637 Thomas, G. E., Olivero, J.J.: Climatology of polar mesospheric clouds 2.  
638 Further analysis of Solar Mesosphere Explorer data, *J. Geophys. Res.*, 96,  
639 14673-14681, doi:10.1029/JD094iD12p14673, 1989.

640

641

642

643

644

645

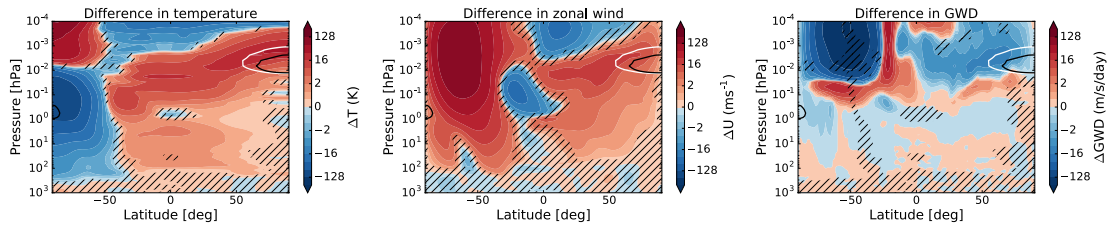
646

647

648

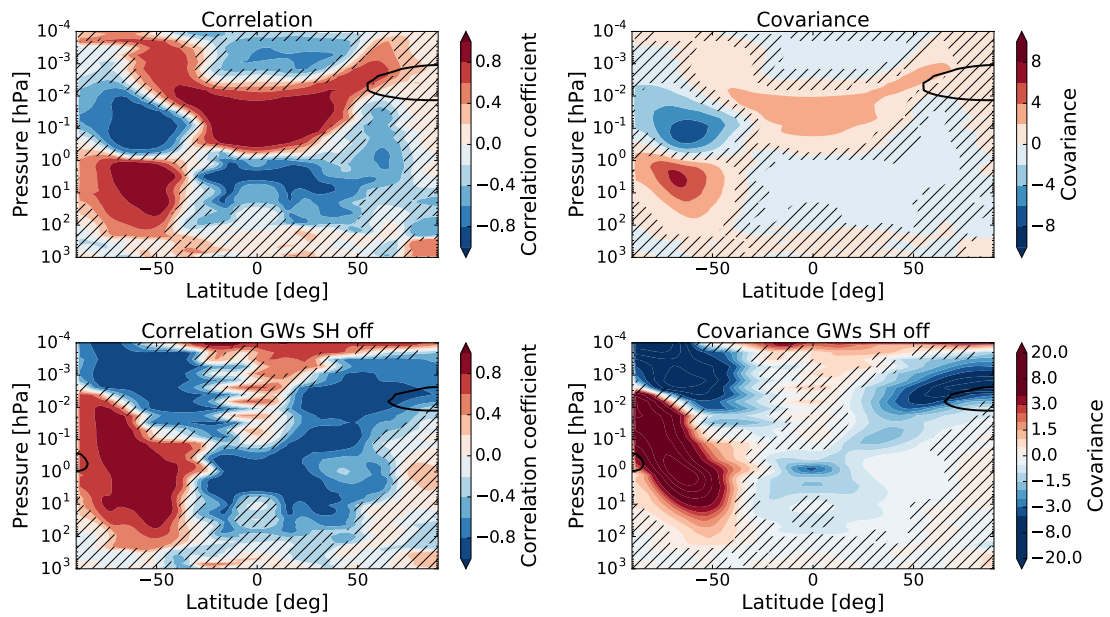
649

650



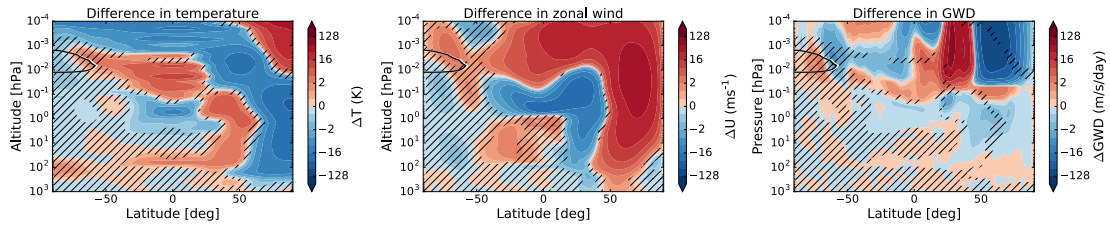
651

652 Fig.1. The difference in zonal-mean temperature (left) and zonal-mean zonal  
 653 wind (right) for July: [run without winter GWs] minus [control run]. The white  
 654 contour indicates the summer polar mesopause region where the  
 655 temperatures are below 150 K for the control run. The black contour indicates  
 656 the region where the temperature is below 150 K for the run without the GWs  
 657 in winter. The shaded areas are regions where the data doesn't reach a  
 658 confidence level of 95%.



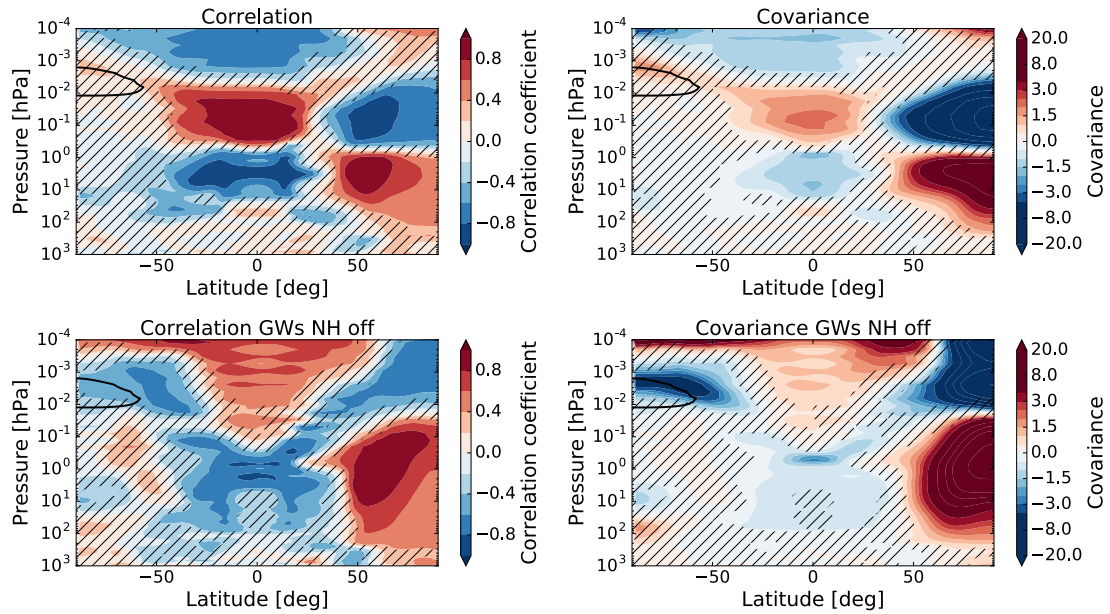
659

660 Fig. 2. The correlation (left) and covariance (right) between the temperature in  
 661 the winter stratosphere (1-10 hPa, 60°S-40°S) and the temperatures in the  
 662 rest of the atmosphere in July for the control run (first row) and run without  
 663 GWs in the winter hemisphere (bottom row). The dotted areas are regions  
 664 where the correlation has a p-value < 0.05. The black 150 K-contour indicates  
 665 the polar mesopause region.



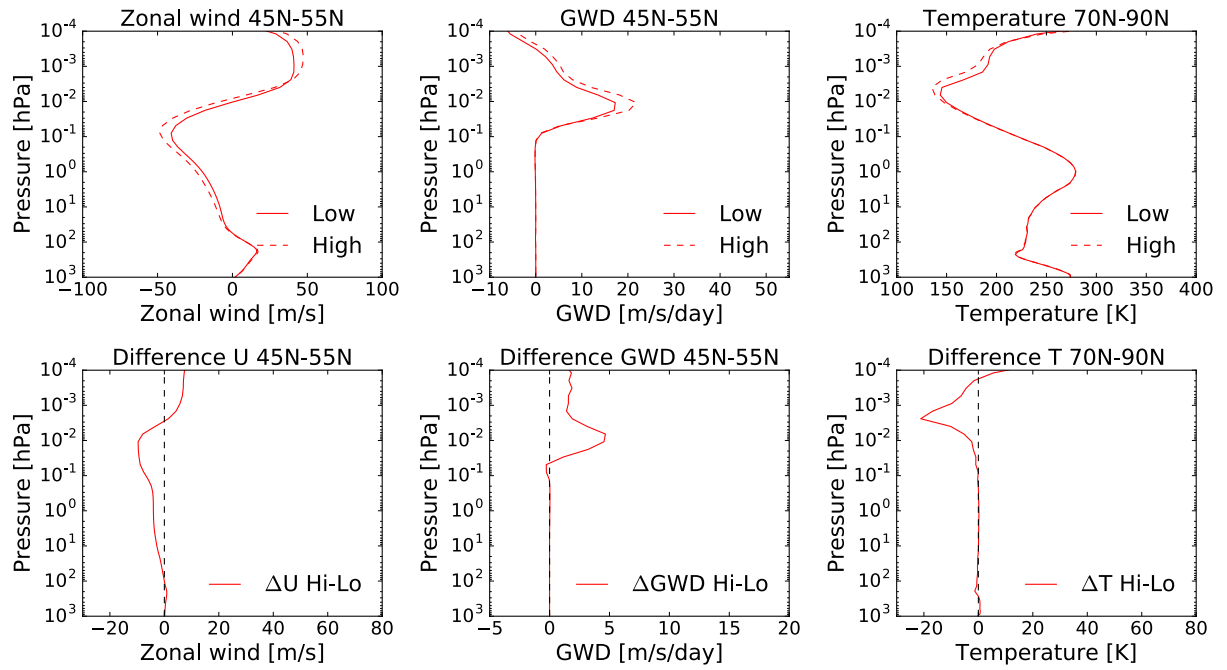
666

667 Fig. 3. Same as Figure 1, but for January.



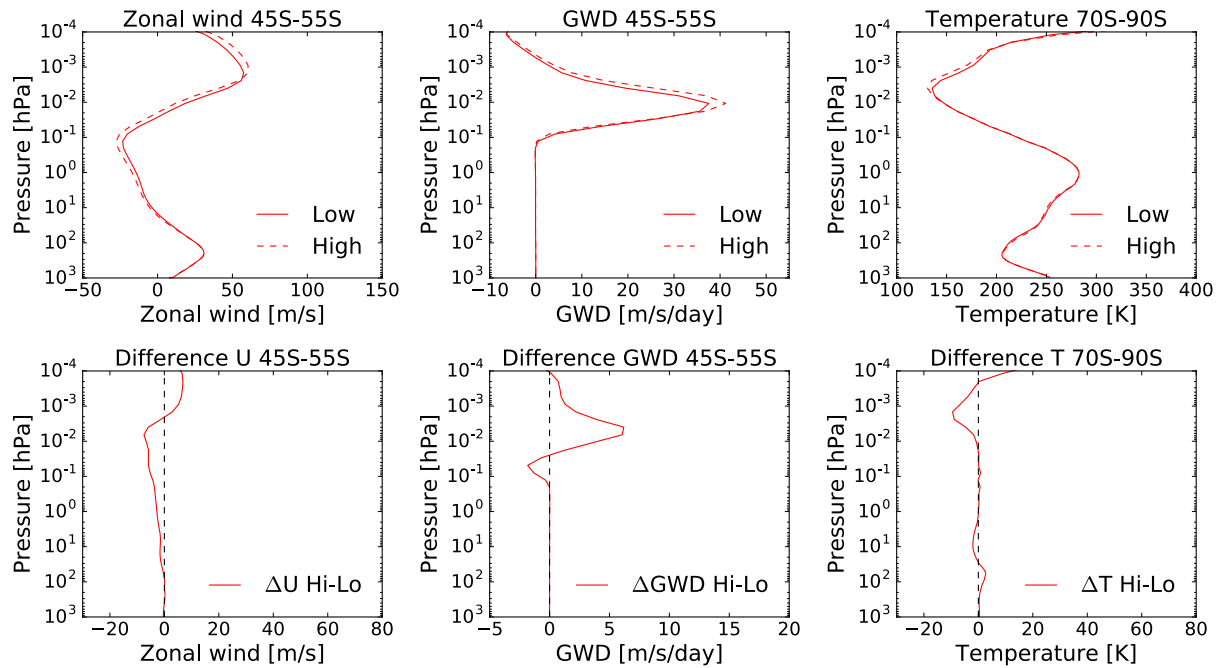
668

669 Fig. 4. The correlation (left) and covariance (right) between the temperature in  
 670 the winter stratosphere (1-10 hPa, 40°N-60°N) and the temperatures in the  
 671 rest of the atmosphere in January for the control run (first row) and run without  
 672 GWs in the winter hemisphere (bottom row). The black 150 K-contour  
 673 indicates the polar mesopause region. The dotted areas are regions where  
 674 the correlation has a p-value < 0.05.



675

676 Fig. 5. The July zonal wind (left) and the GW drag (middle) between 45°-  
 677 55°N and the temperature (right) between 70-90°N for anomalously low and  
 678 high temperatures in the winter stratosphere (1-10 hPa, 60°S - 40°S) (first  
 679 row) and the differences between them (second row), for the case where  
 680 there are no GWs in the winter hemisphere. The red continuous lines show  
 681 the results for anomalously low temperatures, the red dotted lines show the  
 682 results for the anomalously high temperatures.



683

684 Fig. 6. The January zonal wind (left) and the GW drag (middle) between 45°-  
685 55°S and the temperature (right) between 70°S-90°S for anomalously low and  
686 high temperatures in the winter stratosphere (1-10 hPa, 40°N - 60°N) (first  
687 row) and the differences between them (second row), for the case where  
688 there are no GWs in the winter hemisphere. The red continuous lines show  
689 the results for anomalously low temperatures, the red dotted lines show the  
690 results for the anomalously high temperatures.